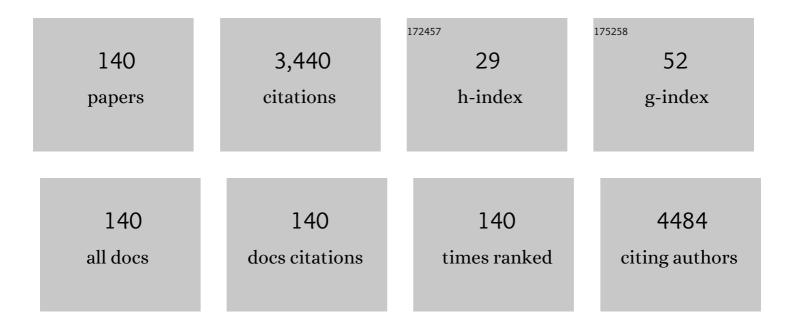
List of Publications by Year in descending order

Source: https://exaly.com/author-pdf/4912277/publications.pdf Version: 2024-02-01



ΒΟΝΑΜΑΓΙ ΡΑΙ

#	Article	IF	CITATIONS
1	Superior adsorptive removal of brilliant green and phenol red dyes mixture by CaO nanoparticles extracted from egg shells. Journal of Nanostructure in Chemistry, 2022, 12, 207-221.	9.1	22
2	Solar irradiated selective nitroaromatics reduction over plasmonic Ag-TiO2: Deposition time dependent size growth and oxidation state of co-catalyst. Chemical Engineering Journal, 2022, 429, 132385.	12.7	8
3	Influence of capping agents on morphology and photocatalytic response of ZnS nanostructures towards crystal violet degradation under UV and sunlight. Separation and Purification Technology, 2022, 281, 119869.	7.9	8
4	Influence of Ag/Cu photodeposition on CaTiO3 photocatalytic activity for degradation of Rhodamine B dye. Korean Journal of Chemical Engineering, 2022, 39, 942-953.	2.7	10
5	Impact of metal ions (Cr ⁺⁶ /Mn ⁺⁷) loaded CaCO ₃ extracted from tap water for adsorption/ degradation of toxic pollutants under sunlight. Materials Express, 2022, 12, 106-113.	0.5	1
6	Recent advances on visible light active non-typical stoichiometric oxygen-rich Bi12O17Cl2 photocatalyst for environment pollution remediation. Journal of Environmental Chemical Engineering, 2022, 10, 107688.	6.7	11
7	Biosynthesized monodispersed spherical Se co-catalyst nanoparticles impregnated over ZnO for 4-chloroguaiacol degradation under solar irradiations. Journal of Environmental Chemical Engineering, 2021, 9, 104892.	6.7	6
8	Preparation and characterization of phase pure monoclinic É'-Bi2O3 nanoparticles and influence of Ni2+and Cu2+ impregnation on their photocatalytic properties. Materials Chemistry and Physics, 2021, 260, 124173.	4.0	14
9	Superior Co-catalysis by Bimetallic Nanostructure for TiO2 Photocatalysis. Journal of Photocatalysis, 2021, 2, 62-70.	0.4	0
10	Superior adsorption removal of dye and high catalytic activity for transesterification reaction displayed by crystalline CaO nanocubes extracted from mollusc shells. Fuel Processing Technology, 2021, 213, 106707.	7.2	18
11	Impact of g-C3N4 loading on NiCo LDH for adsorptive removal of anionic and cationic organic pollutants from aqueous solution. Korean Journal of Chemical Engineering, 2021, 38, 1248-1259.	2.7	24
12	Superior adsorptive removal of eco-toxic drug diclofenac sodium by Zn–Al LDHâ‹xBi2O3 layer double hydroxide composites. Applied Clay Science, 2021, 208, 106119.	5.2	16
13	A review on CaTiO3 photocatalyst: Activity enhancement methods and photocatalytic applications. Powder Technology, 2021, 388, 274-304.	4.2	52
14	Surface structure, morphology and crystal phase-dependent photoactivity of MnO2 nanocatalysts under sunlight. Bulletin of Materials Science, 2021, 44, 1.	1.7	3
15	Enhanced photocatalytic degradation of eco-toxic pharmaceutical waste diclofenac sodium by anion loaded Cu-Al LDHâ‹BiO composites. Journal of the Taiwan Institute of Chemical Engineers, 2021, 129, 227-236.	5.3	8
16	Recent progress in bimetallic nanostructure impregnated metal-organic framework for photodegradation of organic pollutants. Applied Materials Today, 2021, 24, 101105.	4.3	14
17	Role of different oxidation states of Crn+-TiO2 nanocomposites for the degradation of drugs under solar irradiation. Materials Chemistry and Physics, 2021, 269, 124740.	4.0	0
18	Time-dependent growth of CaO nano flowers from egg shells exhibit improved adsorption and catalytic activity. Advanced Powder Technology, 2021, 32, 3288-3296.	4.1	5

#	Article	IF	CITATIONS
19	A brief review on modified layered double hydroxides for H2 production through photoinduced H2O splitting. Environmental Nanotechnology, Monitoring and Management, 2021, 16, 100451.	2.9	2
20	Aloe-vera flower shaped rutile TiO2 for selective hydrogenation of nitroaromatics under direct sunlight irradiation. Arabian Journal of Chemistry, 2020, 13, 2171-2182.	4.9	9
21	Effect of variable oxidation states of Mn+n ion impregnated TiO2 nanocomposites for superior adsorption and photoactivity under visible light. Journal of Alloys and Compounds, 2020, 816, 152639.	5.5	14
22	Morphology Dependent Photocatalytic Activity of CuO/CuO–TiO ₂ Nanocatalyst for Degradation of Methyl Orange Under Sunlight. Journal of Nanoscience and Nanotechnology, 2020, 20, 3123-3130.	0.9	15
23	Photo-induced oxidation and reduction by plasmonic Ag-TiO2 nanocomposites under UV/sunlight. Solar Energy, 2020, 196, 427-436.	6.1	21
24	Morphological influence of ZnO nanostructures and their Cu loaded composites for effective photodegradation of methyl parathion. Solid State Sciences, 2020, 99, 106045.	3.2	22
25	Influence of photodeposition time and loading amount of Ag co-catalyst on growth, distribution and photocatalytic properties of Ag@TiO2 nanocatalysts. Optical Materials, 2020, 106, 109975.	3.6	27
26	Superior co-catalytic activity of Pd(core)@Au(shell) nanocatalyst imparted to TiO2 for the selective hydrogenation under solar radiations. Solar Energy, 2020, 205, 292-301.	6.1	15
27	Solar light driven photocatalytic oxidative degradation of methyl viologen using Mn2+/Mn7+-TiO2 nanocomposites. Journal of Photochemistry and Photobiology A: Chemistry, 2020, 393, 112430.	3.9	10
28	Impact of reducing and capping agents on carbohydrates for the growth of Ag and Cu nanostructures and their antibacterial activities. Particuology, 2019, 43, 219-226.	3.6	21
29	Bimetallic Cu(core)@Zn(shell) co-catalyst impregnated TiO2 nanosheets (001 faceted) for the selective hydrogenation of quinoline under visible light irradiation. Journal of Industrial and Engineering Chemistry, 2019, 79, 314-325.	5.8	16
30	Tuning the band energetics of size dependent titania nanostructures for improved photo-reductive efficiency of aromatic aldehydes. Journal of Industrial and Engineering Chemistry, 2019, 80, 325-334.	5.8	4
31	A co-relation study of efficient photocatalytic reduction of aromatic nitriles and band energies of Cu loaded elongated TiO2 nanocatalysts. Journal of the Taiwan Institute of Chemical Engineers, 2019, 96, 559-565.	5.3	4
32	Influence of co-catalyst amount/size for selective hydrogenation of 1,3-dinitrobenzene over Au-mTiO2 nanocomposites under visible light. Advanced Powder Technology, 2019, 30, 1329-1337.	4.1	8
33	Phase and Shape Dependent Photoactivity of Titania for Nitroaromatics Reduction Under UV Light Irradiation. Journal of Nanoscience and Nanotechnology, 2019, 19, 803-809.	0.9	1
34	Highly efficient CaCO3-CaO extracted from tap water distillation for effective adsorption and photocatalytic degradation of malachite green dye. Materials Research Bulletin, 2019, 116, 1-7.	5.2	20
35	Photodeposition time dependant growth, size and photoactivity of Ag and Cu deposited TiO2 nanocatalyst under solar irradiation. Solar Energy, 2019, 194, 618-627.	6.1	30
36	Fabrication of core–shell PLGA/PLA–pNIPAM nanocomposites for improved entrapment and release kinetics of antihypertensive drugs. Particuology, 2018, 40, 169-176.	3.6	17

#	Article	IF	CITATIONS
37	Catalytic Selective Hydrogenation and Cross Coupling Reaction Using Polyvinylpyrrolidoneâ€Capped Nickel Nanoparticles. ChemistrySelect, 2018, 3, 4738-4744.	1.5	14
38	Oxidative degradation of aliphatic carboxylic acids by photocatalysis with bare and Ag-loaded TiO2 under UV light irradiation. Particulate Science and Technology, 2018, 36, 212-216.	2.1	0
39	Plasmonic stimulated photocatalytic/electrochemical hydrogen evolution from water by (001) faceted and bimetallic loaded titania nanosheets under sunlight irradiation. Journal of Cleaner Production, 2018, 175, 394-401.	9.3	30
40	Synthesis of bimetallic Au-Ag alloyed mesocomposites and their catalytic activity for the reduction of nitroaromatics. Applied Surface Science, 2018, 435, 552-562.	6.1	26
41	Hollow chitosan nanocomposite as drug carrier system for controlled delivery of ramipril. Chemical Physics Letters, 2018, 706, 465-471.	2.6	14
42	Fe ₃ O ₄ @ PLGAâ€PEG Nanocomposite for Improved Delivery of Methotrexate in Cancer Treatment. ChemistrySelect, 2018, 3, 8522-8528.	1.5	11
43	Bimetallic Pd@Ni-mesoporous TiO2 nanocatalyst for highly improved and selective hydrogenation of carbonyl compounds under UV light radiation. Journal of Industrial and Engineering Chemistry, 2018, 67, 486-496.	5.8	15
44	Photodeposition of Ag and Cu binary co-catalyst onto TiO2 for improved optical and photocatalytic degradation properties. Advanced Powder Technology, 2018, 29, 2119-2128.	4.1	36
45	Remarkably Improved Dispersion Stability and Thermal Conductivity of WO3–H2O Suspension by SiO2 Coating. Journal of Nanoscience and Nanotechnology, 2018, 18, 3283-3290.	0.9	4
46	Prediction and optimization of nanoclusters-based thermal conductivity of nanofluids: Application of Box–Behnken design (BBD). Particulate Science and Technology, 2017, 35, 265-276.	2.1	8
47	An investigation into the effect of nanoclusters growth on perikinetic heat conduction mechanism in an oxide based nanofluid. Powder Technology, 2017, 311, 273-286.	4.2	10
48	Highly photoactive Au-TiO2 nanowires for improved photo-degradation of propiconazole fungicide under UV/sunlight irradiation. Solar Energy, 2017, 144, 612-618.	6.1	32
49	A C3N4 surface passivated highly photoactive Au-TiO2 tubular nanostructure for the efficient H2 production from water under sunlight irradiation. Applied Catalysis B: Environmental, 2017, 213, 9-17.	20.2	77
50	Ag + and Cu 2+ doped CdS nanorods with tunable band structure and superior photocatalytic activity under sunlight. Materials Research Bulletin, 2017, 94, 279-286.	5.2	13
51	A Cu+1/Cu0-TiO2 mesoporous nanocomposite exhibits improved H2 production from H2O under direct solar irradiation. Journal of Catalysis, 2017, 346, 1-9.	6.2	66
52	Photo-oxidation kinetics of sugars having different molecular size and glycosidic linkages for their complete mineralization to subunits by bare/Ag–TiO 2 under UV irradiation. Journal of the Taiwan Institute of Chemical Engineers, 2017, 80, 488-494.	5.3	3
53	SiO2-coated pure anatase TiO2 catalysts for enhanced photo-oxidation of naphthalene and anthracene. Particuology, 2017, 34, 156-161.	3.6	13
54	Enhanced co-catalytic effect of Cu-Ag bimetallic core-shell nanocomposites imparted to TiO2 under visible light illumination. Solar Energy Materials and Solar Cells, 2017, 172, 285-292.	6.2	17

#	Article	IF	CITATIONS
55	A Cu-Au bimetallic co-catalysis for the improved photocatalytic activity of TiO2 under visible light radiation. Solar Energy, 2017, 155, 1403-1410.	6.1	25
56	Photocatalytic Degradation of Methylene Blue by Plasmonic Metal-TiO ₂ Nanocatalysts Under Visible Light Irradiation. Journal of Nanoscience and Nanotechnology, 2017, 17, 1210-1216.	0.9	24
57	Effect of time dependent nanoclusters morphology on the thermal conductivity and heat transport mechanism of TiO2 based nanofluid. Heat and Mass Transfer, 2017, 53, 1873-1892.	2.1	6
58	Visible and direct sunlight induced H2 production from water by plasmonic Ag-TiO2 nanorods hybrid interface. Solar Energy Materials and Solar Cells, 2017, 160, 463-469.	6.2	66
59	Effect of Different Shapes of TiO ₂ Nanoparticles on the Catalytic Photodegradation of Salicylic Acid Under UV Light. Journal of Nanoscience and Nanotechnology, 2017, 17, 5303-5309.	0.9	3
60	Selective detection of Mg ²⁺ ions via enhanced fluorescence emission using Au–DNA nanocomposites. Beilstein Journal of Nanotechnology, 2017, 8, 762-771.	2.8	10
61	Core–shell morphology of Au-TiO 2 @graphene oxide nanocomposite exhibiting enhanced hydrogen production from water. Journal of Industrial and Engineering Chemistry, 2016, 37, 288-294.	5.8	28
62	Improved degradation of methyl orange dye using bio-co-catalyst Se nanoparticles impregnated ZnS photocatalyst under UV irradiation. Chemical Engineering Journal, 2016, 306, 1041-1048.	12.7	58
63	Surface structural, morphological, and catalytic studies of homogeneously dispersed anisotropic Ag nanostructures within mesoporous silica. Journal of Nanoparticle Research, 2016, 18, 1.	1.9	6
64	Superior adsorption and photodegradation of eriochrome black-T dye by Fe3+ and Pt4+ impregnated TiO2 nanostructures of different shapes. Journal of Industrial and Engineering Chemistry, 2016, 33, 178-184.	5.8	51
65	Fine CuO anisotropic nanoparticles supported on mesoporous SBA-15 for selective hydrogenation of nitroaromatics. Journal of Colloid and Interface Science, 2016, 461, 203-210.	9.4	24
66	Synthesis and Characterization of Ramipril Embedded Nanospheres of Biodegradable Poly-<1>D,<1>L-Lactide-co-Glycolide and Their Kinetic Release Study. Advanced Science, Engineering and Medicine, 2016, 8, 444-449.	0.3	5
67	Influence of Thermal Treatment and Fe-Loading on Morphology, Crystal Structure, and Photocatalytic Activity of Sodium Titanate Nanotubes. Particulate Science and Technology, 2015, 33, 132-138.	2.1	1
68	Morphological and physicochemical properties of Ag–Au binary nanocomposites prepared using different surfactant capped Ag nanoparticles. RSC Advances, 2015, 5, 39954-39963.	3.6	9
69	Preparation and characterization of different shapes of Au–Ag bimetallic nanocomposites for enhanced physicochemical properties. Colloids and Surfaces A: Physicochemical and Engineering Aspects, 2015, 481, 158-166.	4.7	15
70	Enhanced Photocatalytic Activity of as-Prepared Sodium Titanates for <l>m</l> -Dinitrobenzene Reduction and Sulfosulfuron Oxidation. Journal of Nanoscience and Nanotechnology, 2015, 15, 1490-1498.	0.9	4
71	Shape Dependent Thermal Conductivity of TiO ₂ -Deionized Water and Ethylene Glycol Dispersion. Journal of Nanoscience and Nanotechnology, 2015, 15, 3670-3676.	0.9	2
72	Influence of CuO Nanostructures on the Thermal Conductivity of DI Water and Ethylene Glycol Based Nanofluids. Particulate Science and Technology, 2015, 33, 224-228.	2.1	4

#	Article	IF	CITATIONS
73	Phase-dependent thermophysical properties of α-and γ-Al2O3 in aqueous suspension. Journal of Industrial and Engineering Chemistry, 2015, 25, 99-104.	5.8	6
74	Highly dispersed Au, Ag and Cu nanoparticles in mesoporous SBA-15 for highly selective catalytic reduction of nitroaromatics. RSC Advances, 2015, 5, 184-190.	3.6	42
75	Selective formation of benzo[c]cinnoline by photocatalytic reduction of 2,2′-dinitrobiphenyl using TiO ₂ and under UV light irradiation. Chemical Communications, 2015, 51, 8500-8503.	4.1	17
76	Enhanced Stability, Conductance, and Catalytic Activity of Gold Nanoparticles via Oxidative Dissolution by KMnO ₄ . Particulate Science and Technology, 2015, 33, 159-165.	2.1	4
77	Plasmonic coinage metal–TiO ₂ hybrid nanocatalysts for highly efficient photocatalytic oxidation under sunlight irradiation. New Journal of Chemistry, 2015, 39, 5966-5976.	2.8	45
78	Facile Synthesis of Anisotropic Au Nanostructures by Laser Irradiation and Study of Their Optical and Electrokinetic Properties. Particulate Science and Technology, 2015, 33, 139-144.	2.1	4
79	Influence of Au Photodeposition and Doping in CdS Nanorods: Optical and Photocatalytic Study. Particulate Science and Technology, 2015, 33, 53-58.	2.1	8
80	Influence of Oxidative Etching of Au Nanostructures by KMnO4 on its Surface Morphology, Electro-kinetic Properties and Improved Catalytic Activity. Journal of Industrial and Engineering Chemistry, 2015, 31, 223-230.	5.8	4
81	Influence of Different Reducing Agents on the Ag Nanostructures and Their Electrokinetic and Catalytic Properties. Journal of Nanoscience and Nanotechnology, 2015, 15, 2753-2760.	0.9	4
82	Preparation, Surface and Crystal Structure, Band Energetics, Optoelectronic, and Photocatalytic Properties of Au _{<i>x</i>} Cd _{1â^'<i>x</i>} S Nanorods. ChemPlusChem, 2015, 80, 851-858.	2.8	4
83	Tuning the optical and photocatalytic properties of anisotropic ZnS nanostructures for the selective reduction of nitroaromatics. Chemical Engineering Journal, 2015, 263, 200-208.	12.7	26
84	Cu nanostructures of various shapes and sizes as superior catalysts for nitro-aromatic reduction and co-catalyst for Cu/TiO2 photocatalysis. Applied Catalysis A: General, 2015, 491, 28-36.	4.3	38
85	Physicochemical and catalytic properties of Au nanorods micro-assembled in solvents of varying dipole moment and refractive index. Materials Research Bulletin, 2015, 62, 11-18.	5.2	10
86	Influence of coinage and platinum group metal co-catalysis for the photocatalytic reduction of m-dinitrobenzene by P25 and rutile TiO2. Journal of Molecular Catalysis A, 2015, 397, 99-105.	4.8	31
87	Homogeneous dispersion of Au nanoparticles into mesoporous SBA-15 exhibiting improved catalytic activity for nitroaromatic reduction. Microporous and Mesoporous Materials, 2015, 202, 219-225.	4.4	18
88	Metal ion-TiO ₂ nanocomposites for the selective photooxidation of benzene to phenol and cycloalkanol to cycloalkanone. Journal of Experimental Nanoscience, 2015, 10, 148-160.	2.4	10
89	Improved catalytic activity and surface electro-kinetics of bimetallic Au–Ag core–shell nanocomposites. New Journal of Chemistry, 2015, 39, 304-313.	2.8	25
90	Woolen bun shaped CdS microspheres enfolded 1D nanowires for the superior photooxidation of dyes: A comparative case study. Journal of Molecular Catalysis A, 2015, 396, 15-22.	4.8	7

#	Article	IF	CITATIONS
91	Photodegradation of Imidacloprid Insecticide by Ag-Deposited Titanate Nanotubes: A Study of Intermediates and Their Reaction Pathways. Journal of Agricultural and Food Chemistry, 2014, 62, 12497-12503.	5.2	24
92	Influence of thermal treatment and Au-loading on the growth of versatile crystal phase composition and photocatalytic activity of sodium titanate nanotubes. RSC Advances, 2014, 4, 51342-51348.	3.6	9
93	Stable anatase TiO ₂ formed by calcination of rice-like titania nanorod at 800 °C exhibits high photocatalytic activity. RSC Advances, 2014, 4, 24704-24709.	3.6	12
94	Improved surface properties and catalytic activity of anisotropic shapes of photoetched Au nanostructures formed by variable energy laser exposure. Journal of Molecular Catalysis A, 2014, 395, 7-15.	4.8	6
95	Anisotropic CuO nanostructures of different size and shape exhibit thermal conductivity superior than typical bulk powder. Colloids and Surfaces A: Physicochemical and Engineering Aspects, 2014, 459, 282-289.	4.7	19
96	Sensitivity of the Multiple Functional Moieties of Amino Acids for the Self-Assembly of Au Nanoparticles on Different Physicochemical Properties. Journal of Cluster Science, 2014, 25, 1085-1098.	3.3	1
97	Co-catalytic and electro-kinetic properties of Au nanostructures dispersed in solvents of varying dipole moments. Colloids and Surfaces A: Physicochemical and Engineering Aspects, 2014, 441, 155-163.	4.7	6
98	100% selective yield of m-nitroaniline by rutile TiO2 and m-phenylenediamine by P25-TiO2 during m-dinitrobenzene photoreduction. Catalysis Communications, 2014, 53, 25-28.	3.3	23
99	Superior photoactivity and stability of movable CdS (core)–CdO (shell) nanostructures formed in tubular SiO2 by laser etching of SiO2@CdS nanorod. Chemical Engineering Journal, 2014, 246, 260-267.	12.7	15
100	Core–shell structure of metal loaded CdS–SiO2 hybrid nanocomposites for complete photomineralization of methyl orange by visible light. Journal of Molecular Catalysis A, 2014, 391, 158-167.	4.8	28
101	Shape-dependent bactericidal activity of TiO2 for the killing of Gram-negative bacteria Agrobacterium tumefaciens under UV torch irradiation. Environmental Science and Pollution Research, 2013, 20, 6521-6530.	5.3	23
102	Priority PAHs in orthodox black tea during manufacturing process. Environmental Monitoring and Assessment, 2013, 185, 6291-6294.	2.7	30
103	Polycyclic aromatic hydrocarbons in some grounded coffee brands. Environmental Monitoring and Assessment, 2013, 185, 6459-6463.	2.7	23
104	Photocatalytic degradation of N-heterocyclic aromatics—effects of number and position of nitrogen atoms in the ring. Environmental Science and Pollution Research, 2013, 20, 3956-3964.	5.3	14
105	Highly enhanced photocatalytic activity of Au nanorod–CdS nanorod heterocomposites. Journal of Molecular Catalysis A, 2013, 378, 246-254.	4.8	35
106	Fabrication of hollow SiO2 and Au (core)–SiO2 (shell) nanostructures of different shapes by CdS template dissolution. Journal of Sol-Gel Science and Technology, 2013, 68, 284-293.	2.4	3
107	Study of excited charge carrier's lifetime for the observed photoluminescence and photocatalytic activity of CdS nanostructures of different shapes. Journal of Molecular Catalysis A, 2013, 371, 77-85.	4.8	42
108	Photocatalytic activity of transition metal and metal ions impregnated TiO2 nanostructures for iodine formation. Journal of Molecular Catalysis A, 2013, 371, 48-55.	4.8	23

#	Article	IF	CITATIONS
109	Fine-tuning the photoluminescence and photocatalytic properties of CdS nanorods of varying dimensions. Materials Research Bulletin, 2013, 48, 1403-1410.	5.2	11
110	Co-catalysis effect of different morphological facets of as prepared Ag nanostructures for the photocatalytic oxidation reaction by Ag–TiO2 aqueous slurry. Materials Chemistry and Physics, 2013, 143, 393-399.	4.0	15
111	Highly porous ZnS microspheres for superior photoactivity after Au and Pt deposition and thermal treatment. Materials Research Bulletin, 2013, 48, 4867-4871.	5.2	12
112	The preparation, surface structure, zeta potential, surface charge density and photocatalytic activity of TiO2 nanostructures of different shapes. Applied Surface Science, 2013, 280, 366-372.	6.1	114
113	Selective Photo-Reduction of <l>p</l> -Nitrophenol to <l>p</l> -Aminophenol by Au Deposited CdS Nanostructures of Different Shapes Having Large Surface Area. Journal of Nanoscience and Nanotechnology, 2013, 13, 4917-4924.	0.9	8
114	Superior Photoluminescence and Photocatalytic Activity of CdS (Core)–SiO ₂ (Shell) Nanostructures Obtained by CdS Photoetching and Au Deposition. Journal of Nanoscience and Nanotechnology, 2013, 13, 5069-5079.	0.9	3
115	PHOTOCHEMICAL FABRICATION OF TRANSITION METAL NANOPARTICLES USING CdS TEMPLATE AND THEIR CO-CATALYSIS EFFECTS FOR TiO ₂ PHOTOCATALYSIS. International Journal of Nanoscience, 2013, 12, 1350020.	0.7	Ο
116	EFFECT OF Au AND Pt DEPOSITION AND THERMAL TREATMENT ON THE PHOTOCATALYTIC ACTIVITY OF AS-PREPARED ZnS NANOROD. International Journal of Nanoscience, 2013, 12, 1350032.	0.7	1
117	Rapid photokilling of gram-negative Escherichia coli bacteria by platinum dispersed titania nanocomposite films. Materials Chemistry and Physics, 2012, 136, 21-27.	4.0	7
118	Superior photodecomposition of pyrene by metal ion-loaded TiO2 catalyst under UV light irradiation. Environmental Science and Pollution Research, 2012, 19, 2305-2312.	5.3	13
119	The synthesis, structure, optical and photocatalytic properties of silica-coated cadmium sulfide nanocomposites of different shapes. Journal of Colloid and Interface Science, 2012, 368, 250-256.	9.4	21
120	Size and shape dependent attachments of Au nanostructures to TiO2 for optimum reactivity of Au–TiO2 photocatalysis. Journal of Molecular Catalysis A, 2012, 355, 39-43.	4.8	87
121	Photocatalytic syntheses of azoxybenzene by visible light irradiation of silica-coated cadmium sulfide nanocomposites. Chemical Communications, 2007, , 483.	4.1	68
122	Photocatalytic Preparation of Encapsulated Gold Nanoparticles by Jingle-bell-shaped Cadmium Sulfide–silica Nanoparticles. Topics in Catalysis, 2005, 35, 321-325.	2.8	6
123	Synthesis of metal–cadmium sulfide nanocomposites using jingle-bell-shaped core-shell photocatalyst particles. Journal of Applied Electrochemistry, 2005, 35, 751-756.	2.9	9
124	Photocatalytic Killing of Pathogenic Bacterial Cells Using Nanosize Fe ₂ O ₃ and Carbon Nanotubes. Journal of Biomedical Nanotechnology, 2005, 1, 365-368.	1.1	9
125	Photocatalytic Organic Syntheses: Selective Cyclization of Amino Acids in Aqueous Suspensions. ChemInform, 2004, 35, no.	0.0	0
126	Size and Structure-Dependent Photocatalytic Activity of Jingle-Bell-Shaped Silica-Coated Cadmium Sulfide Nanoparticles for Methanol Dehydrogenation. Journal of Physical Chemistry B, 2004, 108, 18670-18674.	2.6	49

#	Article	IF	CITATIONS
127	Photocatalytic Organic Syntheses: Selective Cyclization of Amino Acids in Aqueous Suspensions. Catalysis Surveys From Asia, 2003, 7, 165-176.	2.6	62
128	Photocatalytic redox-combined synthesis of ?-pipecolinic acid from ?-lysine by suspended titania particles: effect of noble metal loading onÂthe selectivity and optical purity of the product. Journal of Catalysis, 2003, 217, 152-152.	6.2	45
129	Layer-by-layer accumulation of cadmium sulfide core—silica shell nanoparticles and size-selective photoetching to make adjustable void space between core and shell. Journal of Photochemistry and Photobiology A: Chemistry, 2003, 160, 69-76.	3.9	21
130	Preparation of Novel Silicaâ^'Cadmium Sulfide Composite Nanoparticles Having Adjustable Void Space by Size-Selective Photoetching. Journal of the American Chemical Society, 2003, 125, 316-317.	13.7	94
131	Photoinduced Chemical Reactions on Natural Single Crystals and Synthesized Crystallites of Mercury(II) Sulfide in Aqueous Solution Containing Naturally Occurring Amino Acids. Inorganic Chemistry, 2003, 42, 1518-1524.	4.0	25
132	Enhanced photocatalytic activity of highly porous ZnO thin films prepared by sol–gel process. Materials Chemistry and Physics, 2002, 76, 82-87.	4.0	244
133	Photocatalytic activity of transition-metal-loaded titanium(IV) oxide powders suspended in aqueous solutions: Correlation with electron–hole recombination kinetics. Physical Chemistry Chemical Physics, 2001, 3, 267-273.	2.8	192
134	Photocatalytic degradation of o-cresol sensitized by iron–titania binary photocatalysts. Journal of Molecular Catalysis A, 2001, 169, 147-155.	4.8	91
135	Preparation of iron oxide thin film by metal organic deposition from Fe(III)-acetylacetonate: a study of photocatalytic properties. Thin Solid Films, 2000, 379, 83-88.	1.8	111
136	Photodegradation of polyaromatic hydrocarbons over thin film of TiO2 nanoparticles; a study of intermediate photoproducts. Journal of Molecular Catalysis A, 2000, 160, 453-460.	4.8	58
137	Photocatalytic formation of hydrogen peroxide over highly porous illuminated ZnO and TiO ₂ thin film. Toxicological and Environmental Chemistry, 2000, 78, 233-241.	1.2	7
138	Preparation and characterization of TiO2/Fe2O3 binary mixed oxides and its photocatalytic properties. Materials Chemistry and Physics, 1999, 59, 254-261.	4.0	190
139	Photocatalytic degradation of salicylic acid by colloidal Fe2O3 particles. Journal of Chemical Technology and Biotechnology, 1998, 73, 269-273.	3.2	21
140	Enhanced Photocatalytic Activity of Coinage Metal-Cadmium Sulfide Nanorod Composites under Sun Light Irradiation. Advanced Materials Research, 0, 678, 189-192.	0.3	1